388–394 Nucleic Acids Research, 1997, Vol. 25, No. 2

Binding site of the M-domain of human protein SRP54 determined by systematic site-directed mutagenesis of signal recognition particle RNA

Krishne Gowda, Kimberly Chittenden and Christian Zwieb*

Department of Molecular Biology, The University of Texas Health Science Center at Tyler, PO Box 2003, Tyler, TX 75710, USA

Received August 19, 1996; Revised and Accepted October 15, 1996

DDBJ/EMBL/GenBank accession no. U51920

ABSTRACT

The interaction of protein SRP54M from the human signal recognition particle with SRP RNA was studied by systematic site-directed mutagenesis of the RNA molecule. Protein binding sites were identified by the analysis of mutations that removed individual SRP RNA helices or disrupted helical sections in the large SRP domain. The strongest effects on the binding activity of a purified polypeptide that corresponds to the methionine-rich domain of SRP54 (SRP54M) were caused by changes in helix 8 of the SRP RNA. Binding of protein SRP19 was diminished significantly by mutations in helix 6 and was stringently required for SRP54M to associate. Unexpectedly, mutant RNA molecules that resembled bacterial SRP RNAs were incapable of interaction with SRP54M, showing that protein SRP19 has an essential and direct role in the formation of the ternary complex with SRP54 and SRP RNA. Our findings provide an example for how, in eukaryotes, an RNA function has become protein dependent.

INTRODUCTION

Signal recognition particle (SRP) is a cytosolic ribonucleoprotein complex that assists in the co-translational translocation of proteins across lipid bilayers [reviewed by (1)]. Simple bacterial SRPs consist of a 54 kDa polypeptide [SRP54, also named P48 or *ffh*, (2–5)], that is bound to SRP RNA. Mammalian SRPs are composed of a 300 nucleotide RNA (MW 97 142), and the six polypeptides SRP9, SRP14, SRP19, SRP54, SRP68, and SRP72 (6). The prominent role of SRP54 in protein secretion is underscored by its appearance in all phylogenetic groups, its high degree of conservation (7), and its close proximity to the signal peptide (8,9). The M-domain of SRP54 (SRP54M) contains many methionine residues (4,5) believed to bind not only with the SRP RNA (10,11), but also with the signal peptide (12). SRP54M is sufficient for the interaction with SRP RNA (11).

In mammals, protein SRP54 associates with the larger of the two SRP domains (13,14), but only after SRP19 has bound to the SRP RNA (6). Since there are no perceivable interactions between the free SRP19 and SRP54 polypeptides, their assembly appears to be directed by an SRP19-induced conformational change in the RNA (11,15–17). Protein SRP19 may displace SRP RNA helix 6 and uncover the SRP54 binding sites. Alternatively, SRP19 may play a more active role in shaping the SRP54-binding site.

To determine details of the RNP assembly in the human SRP, we measured the binding activities of mutated SRP RNAs toward purified SRP19 and SRP54M. We established that SRP54M binds predominantly to helix 8 of the human SRP RNA, and that the association is strictly dependent on protein SRP19. Furthermore, SRP RNA helix 6 does not interfere sterically with the binding of SRP54M, suggesting that SRP19 plays an intimate role in the formation of the SRP54 binding site.

MATERIALS AND METHODS

Cloning and expression of the M-domain of human SRP54

Oligonucleotides used in PCR reactions, site-directed mutagenesis, or sequencing were synthesized on an Applied Biosystems (PCR-mate) DNA synthesizer (trityl-on) using β-cyanoethyl-phosphoramidite chemistry. Products were purified and detritylated on an oligonucleotide purification cartridge as supplied by the manufacturer. The DNA region corresponding to the M-domain of human SRP54 (amino acid residue position 297–504; GenBank Accession number U51920) was amplified via PCR with oligonucleotides 5′-ACTTCTTGCCATGGGCGACATTGAAG-3′ and 5′-GGAAACCTCGAGGTCTCAGCAAA-3′ as primers and plasmid phSRP54 (Gowda *et al*., unpublished) as template. The PCR product was concentrated by phenol/chloroform extraction and ethanol precipitation, restricted with *Nco*I and *Xho*I (introduced restriction sites are underlined in the primer sequences above), and purified by electrophoresis on 2% agarose gels (18). The expected 681 bp fragment was eluted by centrifugation through 3MM paper and ligated to *Nco*I–*Xho*I-digested DNA of the pET23D expression vector (Novagen). The ligated mixture was transformed into competent *Escherichia coli* DH5-α cells (BRL). DNA from individual transformants were prepared on a small scale, and restricted with *Nco*I and *Xho*I to confirm the presence of correct inserts in the resulting plasmid, phSRP54M. One clone was selected and a polypeptide of the expected molecular weight (23 269 kDa) was expressed in IPTG-treated *E.coli* JM109-DE3 and BL21-DE3 cells (19), as was shown by SDS PAGE of an aliquot of the lysed cells. DNA of phSRP54M was prepared on a large scale from cells grown overnight in a 400 ml culture and purified by CsCl gradient centrifugation (18).

*To whom correspondence should be addressed. Tel: +1 903 877 7689/7676; Fax: +1 903 877 5876; Email: zwieb@jason.uthct.edu

For large scale purification of the SRP54M protein, competent *E.coli* cells (BL21-DE3-pLysS, Novagen) were prepared, freshly transformed with phSRP54M-DNA (20), and incubated overnight at 37°C on 10 cm diameter agar plates containing LB and 100 µg/ml Ampicillin (Sigma) and 37 µg/ml chloramphenicol (Fisher Scientific). Two 2 l Erlenmeyer flasks, each with 400 ml of LB, 100 µg/ml Ampicillin and 37 µg/ml chloramphenicol were inoculated with all colonies from two plates each, and the cultures were grown at 37°C with vigorous shaking for ~45 min until the A_{600} was between 0.5 and 0.8. Both cultures were used to seed a 20 l fermenter (Bioflo IV, New Brunswick Scientific) containing 11.2 l of LB medium (with enough nutrients for 12 l), 240 mg of Ampicillin, 960 mg of Methicillin (USB), 410 mg of chloramphenicol and 1.2 ml of Antifoam 289 (Sigma) kept at 37°C with aeration. The vessel pressure was 20 p.s.i., and the speed of the stirrer was set to 600 r.p.m. Expression of SRP54M was induced when the A_{600} of the culture reached 0.6–0.8 (after ~2.5 h) by adding IPTG (Gold Biotechnologies) to a final concentration of 1 mM, after which growth was continued for 2 h. Cells were subjected to centrifugation for 15 min at 5824 *g* at 4°C (4000 r.p.m. in a Sorvall, H6000 rotor). Approximately 30 g of cells were resuspended in 210 ml of lysis buffer (50 mM $NaPO_4$, pH 8.0, 300 mM NaCl, 5 mM DTT) and frozen at –70°C.

All subsequent manipulations for protein purification were carried out at 4°C. The frozen cells were thawed on ice and sonicated (Fisher, Model 300) at 60% of maximum output using an 'intermediate' tip, for 10 pulses, 15 s each. The lysate was submitted to centrifugation for 10 min at 14 500 *g* (Sorvall SS34, 10 000 r.p.m.). The resulting supernatant was submitted to centrifugation for 4 h at 80 000 *g* (Beckman, VTi 50, 30 000 r.p.m.). The supernatant (~116 ml) was diluted by adding 5 vol of a buffer that contained 50 mM $NaPO_4$, pH 8.0, and 5 mM DTT to reduce the NaCl concentration to 50 mM, and was loaded onto a Biorex 70 (BioRad) cation exchange column (2.5 cm diameter, 28 cm long, total bed volume of 138 ml) equilibrated in 50 mM $NaPO_4$, pH 8.0, 50 mM NaCl, 5 mM DTT (equilibration buffer) and connected to an FPLC system (Pharmacia) at a flow rate of 1 ml/min. The column was washed with 300 ml of equilibration buffer, after which a linear gradient from 50 mM to 1 M NaCl (total gradient volume of 150 ml) was applied in 50 mM $NaPO_4$, pH 8, 5 mM DTT at a flow rate of 1 ml/min. Analysis of aliquots from the collected fractions by SDS PAGE and Coomassie blue G250 staining showed the elution of SRP54M at ~250 mM NaCl and, to a minor degree, at ~305 mM. Fractions from each peak were pooled separately (~9 ml for the weakly-bound material and 21 ml for the strongly-bound material), concentrated to a volume of 2.5 ml by centrifugation at 3500 *g* (Sorvall SS34, 5000 r.p.m.) using Amicon Centricon 10. The protein concentration was determined by a modification of the Bradford (Bio-Rad) protein assay (21) as described (22). The protein was stored at a concentration of 7 mg/ml in 50 mM $NaPO_4$, pH 8.0, 250 mM NaCl, 5 mM DTT, and 50% glycerol at –20°C until further use. Purity of the preparation was determined by densitometric scanning of the Coomassie blue stained gels after SDS PAGE using an Abaton 300/GS scanner and NIH Image software (23).

In vitro synthesis of mutant RNAs

Plasmids coding for authentic human SRP RNA or for mutant RNAs that lacked individual RNA helices was described earlier (17). Mutant ΔH67 was generated by PCR site-directed mutagenesis (24) using oligonucleotide 5′-CGGTTCACCCCTTGCCGAACT-TAGTG-3′ as a mutagenic primer. Details of the construction of other mutations in the large domain of the SRP covering residues 100–252 were communicated previously (25).

T7-polymerase was prepared as described (26) with modifications kindly provided by Arthur Zaug, University of Colorado, Boulder. Plasmids were restricted with *Dra*I, or *Bam*HI (for mutant DNAs of Δ35 and H6), concentrated by phenol–chloroform extraction and ethanol precipitation, and the DNAs were dissolved in 10 mM Tris–HCl, pH 7.5, 1 mM EDTA at a concentration of 1 µg/µl. Run-off transcriptions were carried out for 2 h at 37°C in 200 mM HEPES–KOH, pH 7.5, 30 mM $MgCl_2$, 2 mM spermidine, 40 mM DTT, 6 mM of each rNTP, 0.3–1 µg/µl of restricted DNA, and an amount of T7-polymerase that was optimized to maximize RNA yields. After transcription, 1/10 vol of 0.5 M EDTA, pH 8 and 0.4 vol of 9 M LiCl were added, the samples were incubated on ice for 30 min, and the RNAs were concentrated by centrifugation in a microfuge for 10 min. The pellets were washed with 1 ml of ice-cold 2.5 M LiCl, followed by centrifugation and a wash with 80% ethanol. The pellets were dried and the RNA was dissolved in a small volume of water and stored at –20°C. Transcribed H6-RNAs were precipitated by adding 0.05 vol of 5 M NaCl, 1/10 vol of 0.5 M EDTA, pH 8, and 3 vol of ethanol. Incubation was at –70°C for 30 min, after which the RNA was collected, washed and dissolved in water as described above for the larger RNAs.

The RNA concentrations of the samples were determined by electrophoresis of appropriately diluted sample aliquots on 2% agarose gels followed by staining with ethidium bromide and calculated from a standard curve obtained with known amounts of *E.coli* 5S rRNA (Boehringer) separated on the same gel.

Binding of proteins SRP19 and SRP54M to mutant RNAs

RNAs were incubated in 100 µl binding buffer (50 mM Tris–HCl, pH 7.9, 300 mM KOAc, 5 mM $MgCl_2$, 1 mM DTT and 10% glycerol) at a concentration of 0.4 µg/µl at 60°C for 10 min followed by a gradual cooling to room temperature for ~30 min. Two µl aliquots of purified human protein SRP19 (22) and/or purified human protein SRP54M at appropriate concentrations (see Results) were added by gently mixing with a pipette tip followed by an incubation at 37°C for 10 min. Sequential binding of proteins was carried out by adding 1 µl of SRP54M to the RNA SRP19-complex followed by another 10 min incubation at 37°C.

RNA protein complexes were loaded onto a small (20 µl bed volume) DEAE–Sepharose column prepared in a 200 µl pipette tip (T-200, 0.4 mm, Phenix) with the insert cut from a barrier tip insert (National Scientific), equilibrated in 300 mM KOAc, 50 mM Tris–HCl, pH 7.9, 5 mM $MgCl_2$ and 1 mM DTT. Each column was washed with 200 µl of the equilibration buffer. The flowthrough and the wash were collected in the same tube (F). Bound material (E) was eluted with 200 µl of a buffer containing 1 M KOAc, 50 mM Tris–HCl, pH 7.9, 5 mM $MgCl_2$ and 1 mM DTT. A 1/10th vol of 100% TCA was added to all samples followed by an incubation on ice for 30 min to precipitate the proteins and the RNA protein complexes. The precipitate was collected by centrifugation at room temperature for 10 min, resuspended in 10 µl SDS loading buffer [62.5 mM Tris–HCl, pH 6.8, 2% SDS, 0.5% (v/v) β-mercaptoethanol, 0.00125% (w/v) Bromophenol blue, 10% (v/v) glycerol and 100 mM Tris-base], mixed, and heated for 3 min at 95°C followed by electrophoretic

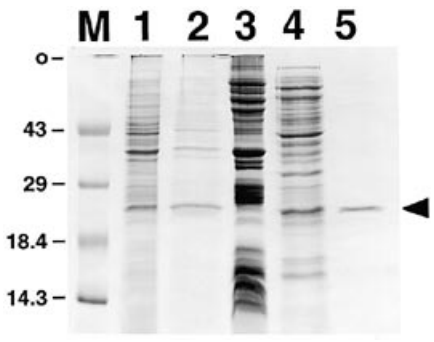

Figure 1. Expression and purification of human SRP54M. Proteins were separated on a linear 15% polyacrylamide SDS gel and stained with Coomassie blue (left). M: Low molecular weight marker (BRL) with protein sizes in kDa. Lane 1: protein extract from uninduced *E.coli* cells; lane 2: protein extract from *E.coli* cells induced with IPTG for 2 h; lane 3: pellet of centrifugation at 80 000 *g*; lane 4: supernatant of centrifugation at 80 000 *g*; lane 5: pooled 250 mM NaCl eluate from Biorex 70 chromatography. The arrowhead indicates the position of protein SRP54M. This polypeptide corresponds to positions 297–504 of human SRP54 (GenBank Accession number U51920).

separation of the polypeptides on 15% polyacrylamide SDS-containing gels. Proteins were stained with Coomassie blue G250, the gel was destained, and scanned electronically without image enhancements. The areas of the peaks were measured using NIH Image software (23).

Display of the large SRP RNA domain

The three-dimensional model of the human SRP RNA structure (27) was obtained from the SRP database (7) in the PDB file-format (28) at the Internet address http://pegasus.uthct.edu/SRPDB/SRPDB.html, and was displayed on an Silicon Graphics Indigo 2 Extreme workstation using the program DRAWNA (29). Experimental data were incorporated into the model by color-coding those mutated sections of the SRP RNA that had significant effects on the binding of proteins SRP19 and SRP54M as described in Results. The model was accepted as provided with no additional structural constraints.

RESULTS

Expression of the M-domain of human SRP54

The M-domain of human SRP54 (SRP54M) corresponding to amino acid residue positions 297–504 of the full-length polypeptide was cloned under control of the bacteriophage T7 promoter by PCR amplification of the corresponding DNA fragment (see Materials and Methods). A soluble polypeptide of the expected size was synthesized in *E.coli* by induction with IPTG. The protein was purified by differential centrifugation and chromatography on Biorex 70 (see Fig. 1, and Materials and Methods). SDS PAGE showed that the majority of SRP54M eluted at 250 mM salt, but ~10% of the protein bound under slightly more stringent conditions (305 mM). Material from both the low- and high-salt fractions actively bound to the Δ35 RNA–SRP19 complex (not

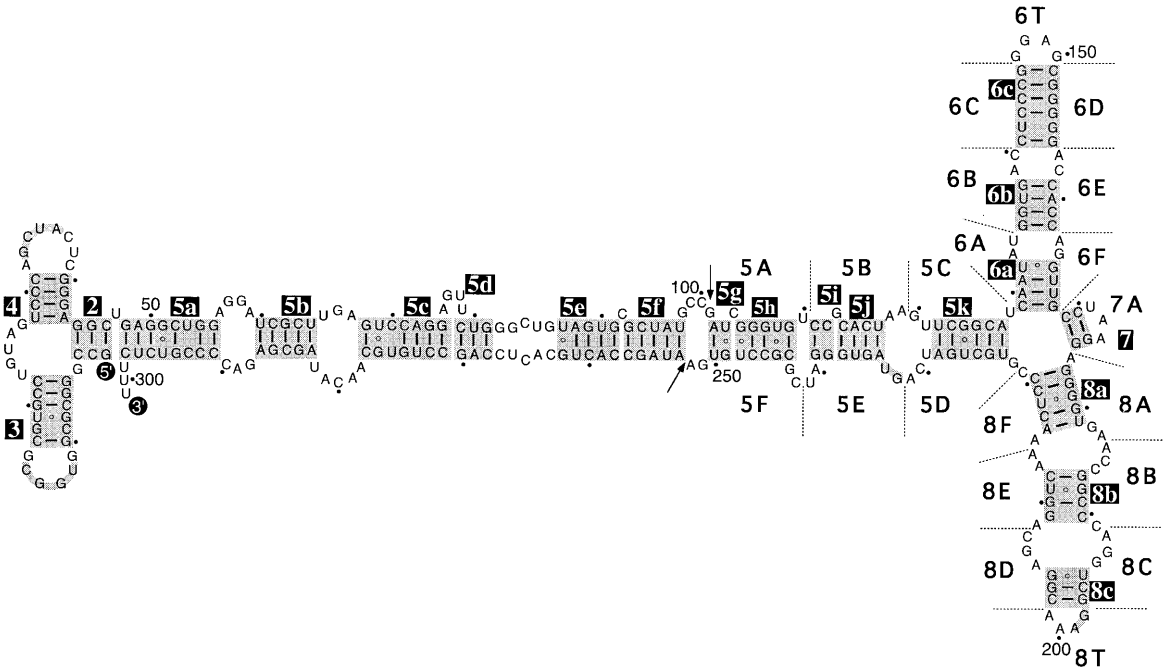

Figure 2. Secondary structure of human SRP RNA. Base pairings are shown as supported by comparative sequence analysis of the SRP RNA sequences compiled in the SRP database (7). The 5′- and 3′-ends of the RNA molecule are labeled as such; helices are marked 2–8 according to the nomenclature of Larsen & Zwieb (30); residues are numbered in 50 nucleotide increments and marked with dots in 10 nucleotide increments; basepaired sections of helices 5, 6 and 8 (highlighted in gray and labeled in reverse print) are given suffices a–k in helix 5, and a–c in helices 6 and 8. Arrows indicate hypersensitive sites cleaved by micrococcal nuclease (34) which separate the large SRP domain (right) from the rest of the particle. The borders between the helix-disrupting mutations (5A–F, 6A–F, 7A, 8A–F) and the two tetraloop mutations (6T and 8T) are indicated by the dotted lines. Each mutation is described in detail in Table 1.

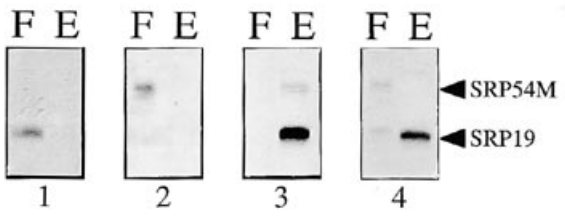

Figure 3. Activities of SRP19 and SRP54M with selected mutant RNAs. Binding activities towards various RNAs were determined in the DEAE assay followed by SDS PAGE as described in Materials and Methods. Proteins in the flowthrough (F) and the eluate (E) are shown. Panel 1: SRP19 with tRNA; panel 2: SRP54M with SRP RNA; panel 3: SRP19 and SRP54M with Δ35 RNA; panel 4: SRP19 and SRP54M with mutant 8E RNA. Under the optimized standardized conditions (see Results) an ~10-fold molar excess of SRP19 over SRP54M was used which explains the relative abundance of protein SRP19.

shown). Scanning of the Coomassie-stained SDS polyacrylamide gels showed that the protein was ~77% pure.

Site-directed mutagenesis of SRP RNA

Nucleotide changes were introduced into the gene for the human SRP RNA in a two-step polymerase chain reaction (PCR) protocol (24,25). This approach allowed us to generate any desired alteration by using only one mutagenic oligonucleotide for each mutant in parallel PCRs. Among the mutations (see Table 1) were a deletion of the small domain (mutant Δ35), deletions of individual RNA helices (mutants ΔH6, ΔH67 and ΔH8), and a mutation that retained only helix 6 (mutant H6). Mutant ΔH67 lacked those nucleotides (positions 128–175) that are absent in the bacterial sequences of a global alignment of SRP RNAs (7,30). The other 22 mutations in the large domain disrupted sections of helices 5–8 (mutants 5A–5F, 6A–6F, 7A and 8A–8F), or compensated the sectional disruptions in helix 6 (mutants C1–C3) by altering both basepaired RNA strands. Two mutants, 6T and 8T, affected the RNA tetranucleotide loops (tetraloops) in helix 6 and helix 8, respectively. (See Table 1 and Figure 2 for the location of the mutations in the secondary structure of the human SRP RNA.) Appropriately restricted template DNAs were used as templates for *in vitro* run-off transcriptions with T7 polymerase to produce RNA molecules of the expected quantity and length (see Materials and Methods).

Mutant RNA binding-activities towards SRP54M or SRP19

The RNAs were activated by renaturation in binding buffer at 60°C followed by slow cooling to room temperature. Purified human SRP54M or SRP19 polypeptides were then added and incubated as described in Materials and Methods. RNA containing material was separated from unbound proteins by chromatography on small DEAE–Sepharose columns. Subsequently, the RNA and RNPs were eluted in a buffer that contained 1 M KOAc. Polypeptides in the flowthrough (F) and the eluate (E) were analyzed by SDS PAGE to determine the degree of binding for each mutant (Fig. 3).

In preliminary binding experiments, we estimated that 4.1 μM human SRP RNA and 2.9 μM SRP19 (standard conditions) were necessary to bind ~95% of purified protein SRP19 (not shown). Under these chosen conditions insignificant amounts of the protein bound to tRNA (Fig. 3, panel 1); to achieve 50% binding of SRP19, ~0.5 μM SRP RNA was required under otherwise

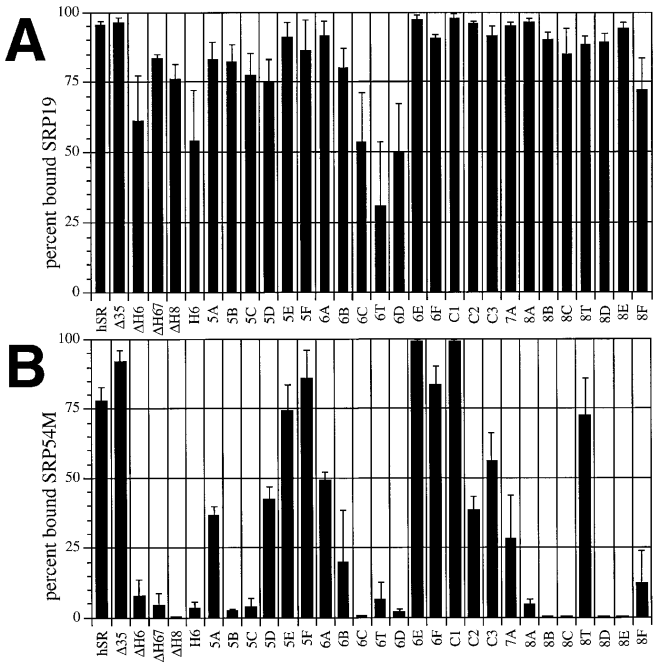

Figure 4. Summary of SRP19 and SRP54M binding activities. Binding activities towards the mutant RNAs were determined in the DEAE assay (see Materials and Methods). (**A**) Activities for protein SRP19; (**B**) percentage of SRP54M bound in the presence of near-saturated amounts of SRP19 (see Results). The height of each bar is calculated from the results of at least three independent experiments. Error bars indicate standard errors of the mean.

identical conditions (not shown). To optimize conditions for ternary complex formation between RNA, SRP19 and SRP54M, we chose Δ35 RNA (8.2 μM), and not SRP RNA, as a substrate. This choice allowed us to account for the greater binding activity of the Δ35 RNA (see Fig. 4B). Using standard conditions for SRP19 binding, we added 0.34 μM of the SRP54M protein preparation to incorporate >95% of SRP54M as judged by scanning of the Coomassie-stained gels (see Materials and Methods).

During the assembly of the large domain of the canine SRP, SRP54 associates with a binary complex composed of SRP RNA and SRP19, but not with naked RNA, nor with isolated protein SRP19. These findings were confirmed with purified human SRP proteins as shown in Figure 3.

To determine if SRP19 simply displaces a portion of the RNA for unmasking of the SRP54M-binding site, we tested the SRP54M binding-activity of all mutant RNAs in the absence of SRP19. We found that none of the RNAs could interact directly with SRP54M, not even at a reduced capacity. Of particular note, two mutant RNAs (ΔH6 and ΔH67) that resemble bacterial SRP RNAs by lacking helix 6, also failed to bind SRP54M when protein SRP19 was omitted (not shown).

Protein SRP19 associated with the majority of the mutant RNAs to various degrees (see Fig. 4A). Within the margin of error, the binding activities of SRP19 were independent of added protein SRP54M, indicating that the dissociation of SRP19 was unaffected by SRP54M. Binding of SRP19 to SRP RNA and Δ35 RNA were identical (96±1.2% and 96±1.8%, respectively), confirming that SRP19 is part of the large SRP domain. Binding was markedly reduced with the RNAs from mutants ΔH6 (61±16%) and ΔH8 RNAs (76±5.4%). Some affinity to a

41-nucleotide RNA-fragment that constitutes helix 6 (mutant H6) was also observed (54±18%). Binding was greatly diminished in mutations that affected the distal portion of helix 6 (mutants 6C and 6D), including the helix 6-tetraloop mutation (6T). Less pronounced, but significant effects on SRP19-binding, were caused by mutants 8C (85±9.2%) and 8F (72±11%), and by some alterations in helix 5 (mutants 5A–5D).

SRP19-dependent binding of SRP54M

To determine SRP54M-binding activities of the mutant RNAs, we added purified SRP54M protein to the pre-formed RNA SRP19 complexes. Mutations with little or no influence on the formation of ternary complex included mutant RNAs Δ35 (92±4.4), 5F (86±10), 6E, (99±1.1%), 6F (83±7.2%) and the compensatory mutation C1 (100%). There were significant reductions in the SRP19 dependent SRP54M binding activities of mutant RNAs 5E (74±9.9%), 6A (50±3.6), C3 (56±11%), 8T (72±14%), but also of the unmutated SRP RNA (77±5.6%) (Fig. 4B). Although RNAs from mutants ΔH8, and 8B–8E bound >75% of the SRP19 polypeptides, they did not associate with detectable amounts SRP54M. In contrast, mutant RNAs ΔH67, 5B, 5C and 8A bound not only some SRP19, but also small amounts of SRP54M (2.2±1.1% to 4.5±2.1%).

Binding sites of SRP19 and SRP54M in the large SRP domain

Examination of the activities of all the RNA mutants suggested that the predominant binding site for SRP19 was located in helix 6 of the large SRP domain. This is supported by the reduced activities of mutants 6C, 6D and the tetraloop mutation 6T (positions 141–156).

Table 1. Character of the SRP RNA mutations

Name	Change	Expected effect on the SRP RNA
hSR	None	None
Δ35	Deletion of nucleotides 1–100 and 252–301	Represents the large SRP RNA domain
ΔH6	Deletion of nucleotides 131–166	Removes helix 6 from the SRP RNA
ΔH67	Deletion of nucleotides 128–175	Removes helices 6 and 7
ΔH8	Deletion of nucleotides 175–222	Removes helix 8
H6	Deletion of nucleotides 1–128 and 169–301	Helix 6 only
5A	103 UCGGGUGU 110 → GUCCGCG	Disrupts a segment of helix 5
5B	111 CCGCACUAA 119 → GGGUGAUG	Disrupts a segment of helix 5
5C	120 GUUCGGCAU 128 → CCAGUCGUG	Disrupts a segment of helix 5
5D	222 GUGCUGAUCA 231 → UACGGCUCGC	Disrupts a segment of helix 5
5E	232 GUAGUGGGAU 241 → AAUCACCCUC	Disrupts a segment of helix 5
5F	242 CGCGCCUG 251 → UUGUGGGU	Disrupts a segment of helix 5
6A	129 CAAUAU 134 → GUUGGA	Disrupts proximal segment of helix 6
6B	135 GGUGAC 140 → CCACCA	Disrupts central segment of helix 6
6C	141 CUCCCG 146 → CGGGGG	Disrupts distal segment of helix 6
6T	147 GGAG 150 → UUCG	Mutates tetraloop of helix 6
6D	151 CGGGGG 156 → GCCCUC	Disrupts distal segment of helix 6
6E	157 ACCACC 162 → CAGUGG	Disrupts central segment of helix 6
6F	163 AGGUUG 168 → UAUAAC	Disrupts proximal segment of helix 6
C1	129 CAAUAU 134 → GUUGGA	
	163 AGGUUG 168 → UAUAAC	Compensates proximal segment of helix 6
C2	135 GGUGAC 140 → CCACCA	
	157 ACCACC 162 → CAGUGG	Compensates central segment of helix 6
C3	141 CUCCCG 146 → CGGGGG	
	151 CGGGGG 156 → GCCCUC	Compensates distal segment of helix 6
7A	169 CC 170 →GG	Disrupts helix 7
8A	176 AGGGGUGA 183 → CCCUCAAG	Disrupts proximal segment of helix 8
8B	184 ACCGGCCC 191 → GAACUGGA	Disrupts central segment of helix 8
8C	192 AGGUCG 197 → CCAGGC	Disrupts distal segment of helix 8
8T	198 GAAA 201 → UUCG	Mutates tetraloop of helix 8
8D	202 CGGAGC 207 → GCUGCA	Disrupts distal segment of helix 8
8E	208 AGGUCAA 214 → CCCGGCC	Disrupts central segment of helix 8
8F	215 AACUCCC 221 → GUGGGGA	Disrupts proximal segment of helix 8

Details of the mutations in comparison with human SRP RNA (hSR) including deletion of individual helices (Δ35, ΔH6, ΔH67, ΔH8 and H6), helix-disrupting and -compensating RNAs (5A–F, 6A–F, 7A–B, 8A–F and C1–C3) with their expected effects on base pairing, and the two tetraloop mutations (6T and 8T).

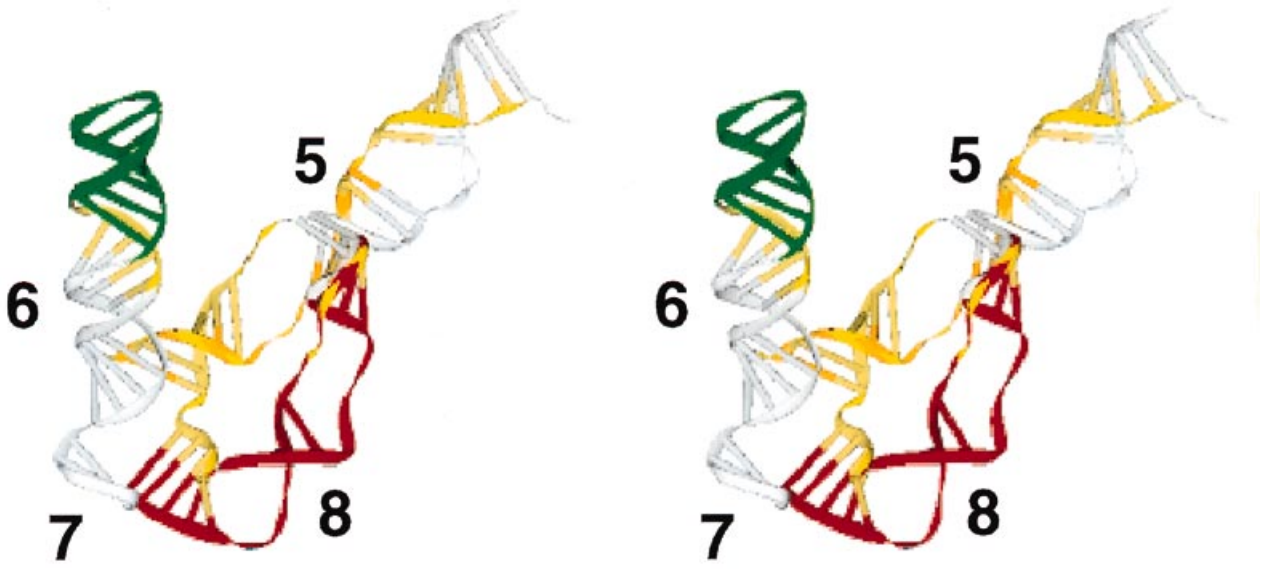

Figure 5. Binding sites for SRP19 and SRP54M in a three-dimensional model of the structure of human SRP RNA. The relaxed stereo view of the large SRP domain was generated as described in Materials and Methods and in (27). Shown are the folded backbone and the paired bases. SRP RNA helices 5–8 are labeled as such. The effects of the mutations on the binding of protein SRP19 are shown in green for pronounced mutational effects (<65% of SRP19 was bound), and yellow, for mild effects (<85%, but >65% of binding). Influences on the RNA binding activities of SRP54M are shown in red for the strong effects, defined either as a complete loss of RNA binding activity for SRP54M at >75% binding of SRP19, or as <5% binding of SRP54M at a >95% binding of SRP19. Mild effects of the mutant RNA, shown in orange, bound <5% of SRP54M at between 60 and 95% binding of SRP19. Other regions of the RNA, coded in grey, were considered to affect protein binding indiscernibly.

Binding to SRP54M was completely abolished when helix 8 was deleted, or when the central and distal portions of helix 8 were altered (mutants 8B, 8C, 8D and 8E). Therefore, we considered most of helix 8, namely positions 176–197 and 202–214, as the predominant binding site of SRP54M. The slightly reduced binding to mutant 8T RNA (72±14%) is explained by its somewhat lower capacity to associate with protein SRP19 (88±3.5%); therefore, the apical GAAA-tetraloop of helix 8 was unlikely to be in contact with SRP54M.

To visualize the binding sites of the two proteins in the context of the assembled SRP, we incorporated the results from the site-directed mutagenesis experiments into a model of the three-dimensional structure of the SRP RNA, proposed previously (27). Our model is characterized by a 'straight' helix 6, and a 'bent' helix 8 that is caused by a hypothetical tertiary interaction between the helix 8 tetraloop and helix 5 (198-GA-199 with 232-GU-233 in the human SRP RNA). Figure 5 shows a color coded view of the large domain with strong and mild mutational effects on the binding of SRP19 and SRP54M. Colors appear only in those regions of the RNA where mutations had a conspicuous impact on protein binding. (The criteria for the classification of the protein binding activities are described in the legend to Figure 5.) Separate binding sites were supported by the complete separation of the strong mutational effects for SRP19 and SRP54M.

The locations of auxiliary binding determinants, or of sites that may also alter the RNA conformation at neighboring sites, were indicted by the mild effects. We found that these mutations were located in helix 5 where they influenced binding of both proteins (positions 111–128 for SRP54M; positions 103–128 and 222–231 for SRP19). Binding of SRP19 was also mildly affected by changes at positions 135–140 in helix 6 and at 192–197 in helix 8. The reduced activity caused by the latter mutant (8C) provided the only example where a mild mutational effect on SRP19 coincided with a strong effect on SRP54M binding.

DISCUSSION

RNA site-directed mutagenesis was used to identify binding sites for proteins SRP19 and SRP54M on the SRP RNA. Since an RNA that corresponded to the large domain of the SRP (mutant Δ35) was fully active in binding both polypeptides, the detailed mutational analysis was confined to a portion of helix 5, and to helices 6, 7 and 8 (Fig. 2). Compensatory mutations that preserved base pairing were introduced only in helix 6, because it is a more-or-less continuous RNA stack that lacks pronounced internal loops.

Most of the SRP RNA mutations (with the exception of mutant ΔH67), had been used earlier with radioactively labeled protein SRP19 translated *in vitro* in a wheat germ cell-free system (17,25). In those experiments, binding of an unknown amount of SRP19 was measured with the respective mutant RNAs in excess. Furthermore, the samples contained an undefined mixture of components including constituents from the wheat germ SRPs. Despite these impediments, the earlier findings agree well with results obtained in a defined system. In both cases, helix 6 was found to be the major binding site for protein SRP19 with a preference for the tetraloop and the 5′-portion of the helix. The influence of the distal portion of helix 8 on SRP19 binding (e.g. mutant 8C) was confirmed. In addition, we now found mild effects caused by mutations throughout helix 5; of those, only mutant 5C was shown previously to have an effect.

There was a small but very reproducible (n = 11) difference in the affinities of SRP54M for SRP RNA (77±5.6%) and the Δ35 RNA (92±4.4%). This result may be explained by interactions

between the small and the large SRP domains. Although we do not know which site of the small domain may cause this effect, in the large domain, nucleotides located at the 3′-side of helix 6 appear involved, as evidenced by the undiminished binding capacity of mutants 6E and C1 (Fig. 4B).

The lower affinity of the unmutated SRP RNA and most mutant RNAs may result from incomplete localized renaturation. However, this interpretation does not explain the high affinities of mutants 6E and C1. Furthermore, when we analyzed conformational differences between the SRP RNA and the various mutant RNA by electrophoresis on non-denaturing polyacrylamide gels, we found no correlation of the binding affinity with the appearance of unfolded molecules (not shown).

SRP RNA helix 8, which is conserved in all SRPs, was identified as the major binding site for SRP54. This result confirmed experimentally what was expected from the comparative sequence analysis of the bacterial SRP components (7,30). Enzymatic and chemical probing showed that P48, the bacterial homologue of SRP54, protects a region in 4.5S RNA that is equivalent to helix 8 of the eukaryotic SRP RNA (31). In the *Mycoplasma mycoides* SRP, P48 protected helix 8 from digestion by RNase A (32). In addition, translocation of nascent polypeptides was promoted by a heterologous complex that consisted of mammalian SRP54 and bacterial 4.5S RNA (33).

Our results show that the human SRP RNA has lost the ability to bind to SRP54M when SRP19 is absent. Surprisingly, none of the mutant RNA molecules, including mutants ΔH6 and ΔH67 which lack helix 6 and thereby closely resemble the bacterial 4.5S RNA, bound even trace amounts of SRP54M. This would have been expected if protein SRP19 simply displaces SRP RNA helix 6 and uncovers a preexisting SRP54 binding sites. A full-length SRP54 polypeptide that we expressed in *E.coli* and insect cells (unpublished results) was incapable of binding to ΔH67 RNA, demonstrating that the G-domain of SRP54 cannot restore the RNA binding activity (not shown).

We conclude that SRP19 is involved fundamentally in the assembly of the SRP by actively shaping the binding site of SRP54. A process is favored whereby SRP19 configures helix 8 as is evidenced by the ability of the protein to influence the distal portion (mutant 8C). However, upon SRP19's interaction with RNA, the SRP54M binding site may be composed of nucleotide and amino acid residues. Thus, the sequential assembly of SRP19 and SRP54 in the large SRP domain provides a compelling example for the increased complexity of the eukaryotic SRP and for an RNA function being 'taken over' by proteins.

ACKNOWLEDGEMENTS

We thank Shaun D. Black for critical reading of the script and Kerfoot P. Walker III for exceptional technical help. This work was supported by NIH grant GM-49034 to C.Z.

REFERENCES

1 Lütcke, H. (1995) *Eur. J. Biochem.*, **228**, 531–550.
2 Poritz, M. A., Bernstein, H. D., Strub, K., Zopf, D., Wilhelm, H. and Walter, P. (1990) *Science*, **250**, 1111–1117.
3 Ribes, V., Römisch, K., Giner, A., Dobberstein, B. and Tollervey, D. (1990) *Cell*, **63**, 591–600.
4 Bernstein, H. D., Poritz, M. A., Strub, K., Hoben, P. J., Brenner, S. and Walter, P. (1989) *Nature*, **340**, 482–486.
5 Römisch, K., Webb, J., Herz, J., Prehn, S., Frank, R., Vingron, M. and Dobberstein, B. (1989) *Nature*, **340**, 478–82.
6 Walter, P. and Blobel, G. (1983) *Cell*, **34**, 525–533.
7 Larsen, N. and Zwieb, C. (1996) *Nucleic Acids Res.*, **24**, 80–81.
8 Krieg, U., Walter, P. and Johnson, A. (1986) *Proc. Natl. Acad. Sci. USA*, **83**, 8604–8608.
9 Kurzchalia, T., Wiedman, M., Girshovich, A., Bochkareva, E., Bielka, H. and Rapoport, T. (1986) *Nature*, **320**, 634–636.
10 Zopf, D., Bernstein, H. D., Johnson, A. E. and Walter, P. (1990) *EMBO J.*, **9**, 4511–4517.
11 Römisch, K., Webb, J., Lingelbach, K., Gausepohl, H. and Dobberstein, B. (1990) *J. Cell Biol.*, **111**, 1793–1802.
12 Lütcke, H., High, S., Römisch, K., Ashford, A. J. and Dobberstein, B. (1992) *EMBO J.*, **11**, 1543–1551.
13 Andrews, D., Walter, P. and Ottensmeyer, P. (1987) *EMBO J.*, **6**, 3471–3477.
14 Siegel, V. and Walter, P. (1988) *Proc. Natl. Acad. Sci. USA*, **85**, 1801–1805.
15 Zwieb, C. (1985) *Nucleic Acids Res.*, **13**, 6105–6124.
16 Zwieb, C. and Ullu, E. (1986) *Nucleic Acids Res.*, **14**, 4639–4657.
17 Zwieb, C. (1991) *Nucleic Acids Res.*, **19**, 2955–2960.
18 Maniatis, T., Fritsch, E. and Sambrook, J. (1982) *Molecular Cloning: A Laboratory Manual*, Cold Spring Harbor Laboratory, Cold Spring Harbor, NY.
19 Studier, F. W., Rosenberg, A. H., Dunn, J. J. and Dubendorff, J. W. (1990) *Methods Enzymol.*, **185**, 60–89.
20 Dagert, M. and Ehrlich, S. (1979) *Gene*, **6**, 23–28.
21 Bradford, M. (1976) *Anal. Biochem.*, **72**, 248–254.
22 Walker, P., Black, S. and Zwieb, C. (1995) *Biochemistry*, **34**, 11989–11997.
23 Rasband, W. (1994) The NIH Image program is in the public domain and available by Anonymous FTP from zippy.nimh.nih.gov.
24 Nelson, R. M. and Long, G. L. (1989) *Anal. Biochem.*, **180**, 147–151.
25 Zwieb, C. (1992) *J. Biol. Chem.*, **267**, 15650–15656.
26 Butler, E. and Chamberlin, M. (1982) *J. Biol. Chem.*, **257**, 5772–5778.
27 Zwieb, C., Müller, F. and Larsen, N. (1996) *Folding & Design*, **1**, 315–324.
28 Bernstein, F., Koetzle, T., Williams, G., Meyer EF, J., Brice, M., Rodgers, J., Kennard, O., Shimanouchi, T. and Tasumi, M. (1977) *J. Mol. Biol.*, **112**, 535–542.
29 Massire, C., Gaspin, C. and Westhof, E. (1994) *J. Mol. Graphics*, **12**, 201–206.
30 Larsen, N. and Zwieb, C. (1991) *Nucleic Acids Res.*, **19**, 209–215.
31 Lentzen, G., Moine, H., Ehresmann, C., Ehresmann, B. and Wintermeyer, W. (1996) *RNA*, **2**, 244–253.
32 Samuelsson, T. (1992) *Nucleic Acids Res.*, **20**, 5763–5770.
33 Hauser, S., Bacher, G., Dobberstein, B. and Lütcke, H. (1995) *EMBO J.*, **14**, 5485–5493.
34 Gundelfinger, E. D., Krause, E., Melli, M. and Dobberstein, B. (1983) *Nucleic Acids Res.*, **11**, 7363–7374.